Colloid Polym Sci (2009) 287:705–713
DOI 10.1007/s00396-009-2017-0

ORIGINAL CONTRIBUTION

PVP superabsorbent nanogels

Vânia B. Bueno · Iolanda M. Cuccovia · Hernan Chaimovich · Luiz H. Catalani

Received: 12 January 2009 / Revised: 11 February 2009 / Accepted: 11 February 2009 / Published online: 4 March 2009

Abstract Monomer free hydrogel nanoparticles (nanogels) were prepared by crosslinking preformed poly(*N*-vinyl-2-pyrrolidone) (PVP) entrapped in the aqueous pool of hexadecyltrimethylammonium bromide reverse micelles using the Fenton reaction. The PVP nanoparticles were spherical with a dry diameter of 27 nm. The diameter of the swollen particles was ten times higher, i.e., a swelling ratio, *Q*, above 900, characterizing this preparation as superabsorbent. PVP nanogel swelling was dependent on bound Fe^{3+} and varied with pH and ionic strength. Nanogel deswelling by salt followed the anions lyotropic series, i.e., $SCN^- < HSO_3^- < NO_3^- < I^- < Cl^- < CH_3COO^- < CF_3SO_3^-$. The value of *Q* reached 6,000 in iron-free PVP nanoparticles at low pH, making this nanogel one of the most efficient swelling systems so far described.

Keywords Superabsorbent nanogel · Reversed micelles · PVP hydrogel · Fenton reaction

Introduction

Hydrogels, biomaterials formed by tridimensional networks of hydrophilic polymers, absorb large amounts of water [1]. Hydrogel nanoparticles are of interest due to their size and biocompatibility [2–4]. Potential applications of nanogels, mainly those with the ability of react to stimulus [5, 6], include their use as drug delivery systems [7–10].

Nanogels can be prepared using a variety of methods, but those prepared with synthetic polymers have been obtained almost exclusively by polymerization of vinylic monomers with crosslinkers, using emulsions, microemulsions, and micelles as templates [11–13]. The use of vinylic monomers is of limited utility for biocompatible applications due to the unavoidable presence of residual highly toxic vinylic monomer. The use of preformed polymers that avoid the use of monomers for nanogel preparation by cross linking has not been explored extensively [14, 15].

Hydroxyl radicals, produced by the Fenton reaction in the presence of poly(*N*-vinyl-2-pyrrolidone) (PVP), generate macroradicals, which, upon collapse, rapidly crosslink the polymer, forming hydrogels of excellent mechanical properties [16, 17]. The hydrogel thus produced is biocompatible and shows no toxicity [17].

Here, we describe a new method for nanogel preparation using the Fenton reaction and hexadecyltrimethylammonium bromide (CTAB) reverse micelles in *n*-hexanol/isooctane as templates. This methodology permitted crosslinking of preformed PVP, thus avoiding residual monomer. The nanogel was characterized by measuring swelling with the lyotropic series of anions, effects of ionic strength, and pH on swelling, morphology and crosslinking density. Under several conditions, we obtained high swelling ratios, up to 6,000, characterizing a remarkable superabsorbancy capacity. Residual Fe^{3+} ions from the Fenton process provided additional swelling control through complexation crosslinking. The major applications envisioned for these

V. B. Bueno · L. H. Catalani (✉)
Departamento de Química Fundamental, Instituto de Química,
Universidade de São Paulo,
CP 26077, 05513-970 São Paulo, Brazil
e-mail: catalani@usp.br

I. M. Cuccovia · H. Chaimovich
Departamento de Bioquímica, Instituto de Química,
Universidade de São Paulo,
CP 26077, 05513-970 São Paulo, Brazil

nanospheres are drug delivery and embolotherapy controlled by ionic strength changes.

Experimental section

PVP (Plasdone K90, M_w=1,300,000) was kindly donated by BASF. Isooctane, *n*-hexanol, and diethyl ether were obtained from Merck, BDH, and Synth (Brazil), respectively. Analytical grade $NaClO_4$, iodine, and KI were from Merck. $FeCl_2$, $FeCl_3$, and H_2O_2 30% was from Aldrich. CTAB was obtained from Acros Organics and used after recrystallization (×3) from acetone/methanol 9:1 (*v*/*v*). All solvents were distilled before use and water was deionized.

The dye poly[(*N*-vinyl-2-pyrrolidone)-*co*-(9-vinyl-anthracene)] (PVPVAn) was synthesized as follows: The polymerization reaction was performed using *N*-vinyl-2-pyrrolidone (VP) and 9-vinyl-anthracene (VA) as monomers (VP/VA ratio=1,000:1 *w*/*w*) and 2,2′-azobis(isobutyronitrile) as initiator (0.1% *w*/*w*) at 70°C for 48 h. Its M_w was determined as 1×10^5 by SEC analysis, against PEO standards. For anisotropy measurements, PVP and PVPVAn were used as a mixture of 1:1 (*w*/*w*).

The PVP nanoparticles were obtained as described in Scheme 1. A solution (21.6 mL) containing 100 g×L^{-1} of PVP and 7 mmol×L^{-1} of $FeCl_2$ was added to 200 mL of a mixture of isooctane/*n*-hexanol (9:1) containing 0.1 mol×L^{-1} of CTAB to set W/S ratio 60. After surfactant dissolution and total clarification by stirring, H_2O_2 in diethyl ether was added to a final concentration of 100 mmol×L^{-1} relative to the water volume. The solution was stirred overnight at room temperature (25±4°C), and the organic phase was removed in a rotary vacuum evaporator. To the resultant aqueous phase, $NaClO_4$ 3 mol×L^{-1} was added to reach a 3:1 mole ratio of ClO_4^-/CTA^+ to precipitate the surfactant. The suspension was centrifuged (15 min, 10,000×*g*), and the supernatant was collected and freeze-dried. To this, saturated NaCl solution was added to coagulate the PVP nanoparticles. The supernatant was separated by decantation, and the resulting solid was re-suspended in water, exhaustively dialyzed, and freeze-dried, yielding a yellow powder. The PVP concentration in the organic phase was estimated using the Lugol method [18]. Typically, 2 g of KI and 1 g of I_2 were dissolved in 300 mL of water. This solution (15 mL) was diluted in 1 L of acetate buffer 5 mmol×L^{-1}, pH4.75. The PVP complex with Lugol Reagent (PVP-I_3^-) was obtained by mixing the PVP solution and the I_3^- solution. This complex absorbs at 400 nm, and the PVP concentration was obtained using appropriate calibration.

The extraction of residual Ferric ions in the nanogel was done by suspending the nanogels in dilute H_3PO_4, followed by successive dialysis with HCl 0.01 mol×L^{-1} and distilled water.

Anisotropy values, Γ, were calculated from fluorescence polarization experiments by Eq. 1 [19].

$$\Gamma = \frac{I_{VV} - I_{VH}\frac{I_{HV}}{I_{HH}}}{I_{VV} + 2I_{VH}\frac{I_{HV}}{I_{HH}}} \tag{1}$$

where I_{VV} is the vertically polarized excitation and vertically polarized emission, I_{VH} is the vertically polarized excitation and horizontally polarized emission, I_{HV} corresponds to the horizontally polarized excitation and vertically polarized emission, and I_{HH} is the horizontally polarized excitation and horizontally polarized emission. Fluorescence intensity was determined using a Spex-Fluorolog-2 model FL-111 fluorometer equipped with an L-format polarization assembly and Glan–Thompson polarizers, model 1935B. Excitation wavelength was 360 nm and emission was detected at 417 nm.

The swelling ratio, Q, (swelling relative to dry state) was calculated using Eq. 2 [20],

$$Q = \frac{w_s - w_d}{w_d} \approx \frac{V_s \times d_w}{V_d \times d_{PVP}} = \left(\frac{D_s}{D_d}\right)^3 \times \frac{d_w}{d_{PVP}} \tag{2}$$

where w_s and w_d are swollen and dry weight of the hydrogel, V_s and V_d are the swollen and dry volume, and d_w

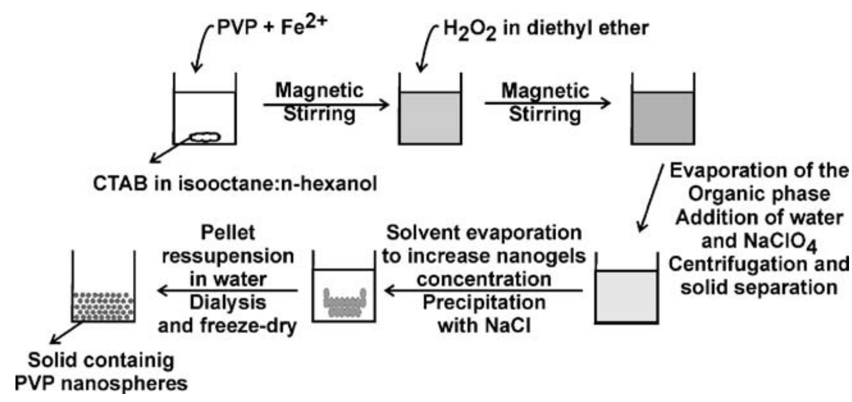

Scheme 1 PVP nanogel preparation

and d_{PVP} are water and PVP densities at 25 °C, respectively (d_{PVP}=1.20 g×mL^{-1}) [21].

The Q/Q_o ratio corresponds to swelling relative to distilled water (Eq. 3):

$$\frac{Q}{Q_0} = \left(\frac{D_S}{D_{S_0}}\right)^3 \quad (3)$$

where Q and Q_0 are the swelling ratios for the swollen states in any solution and in distilled water, respectively, relative to the dry state.

Microscopy images of nanogels were acquired in a scanning electron microscope equipped with a field emission gun (FEG-SEM, model FEG 7401F, from Jeol). Swollen particles were submitted to freeze drying prior to SEM analysis in order to retain morphology [22]. The images were acquired without prior coating, using voltages of 1 and 5 kV and WD near 8 mm. Diameters obtained from SEM images were calculated using AxioVision V. 4.6.3.0 program, by measuring randomly >400 spheres.

Nanogels were swollen in aqueous salt solutions, varying the salt concentration (NaCl) from 0 to 3.8 mol×L^{-1} and varying the anion of sodium salts (triflate, acetate, iodine, nitrate, bisulphite, and tiocianate), in a fixed concentration (0.2 mol×L^{-1}). The hydrodynamic diameter (D_h) was measured by dynamic light scattering using a Dynamic Light Scattering Spectrometer (Brookhaven Instruments, using ZetaPALS Particle Sizing Software Version 2.29). Zeta Potential was measured using a ZetaSizer Nanoseries apparatus (Nano ZS ZEN3600, from Malvern Instruments), at pH 6.5. Nanogel composition was analyzed by ^{1}H NMR, in a Bruker AC200 spectrometer. Residual concentration of Fe ions was determinate by ICP-AES, in a Spectro Cirus CCD apparatus. Turbidity measurements were performed with a spectrophotometer Shimadzu Multispec-1501, in the transmittance mode (400 nm), using Eq. 4 [23]:

$$\tau = d \ln\left(\frac{I_0}{I}\right) \quad (4)$$

where τ is turbidity (in turbidity units), d is the optical path length, and I and I_0 are the transmittances of the solution and the reference, respectively.

Results

PVP dissolved readily in n-hexanol/isooctane (1:9 v/v) containing CTAB (0.1 mol×L^{-1}; W/S=60) yielding transparent solutions, but remained insoluble in the solvent mixture alone, indicating that PVP was included in the aqueous pool of the reverse micelles. The increase in the D_h observed upon polymer addition also indicated that PVP was incorporated in the micellar aqueous compartment (Table 1).

In order to attain Fenton reaction conditions, $FeCl_2$ was added to the PVP aqueous solution prior to micelle inclusion. The addition of $FeCl_2$ or $FeCl_3$ did not significantly change the PVP solubility in the micellar system. Micelles containing Fe ions and PVP exhibited diameters higher than those with PVP alone (Table 1). Ferrous and ferric ions form stable complexes with PVP [24], conferring a polyelectrolyte character to the polymer. We attribute the ion-induced diameter increase to intramolecular charge–charge repulsion.

Fe^{2+}-containing PVP in reverse micelles was crosslinked by addition of H_2O_2. The micelles containing crosslinked PVP were smaller than those micelles containing non crosslinked PVP/$FeCl_3$ or only PVP (Table 1). Volume reduction upon crosslinking, which may be more prominent in nanosized structures, is a known nanogel property. [25].

The ^{1}H NMR spectrum of purified, detergent-free hydrogel PVP nanospheres (see “Experimental section”) was identical of that of pure crosslinked PVP. CTAB NMR peaks were absent (not shown), indicating that the surfactant had been totally removed.

The initial (added) iron concentration was 8.9 mg of Fe/g PVP. Iron concentration in the final purified nanospheres was 6.8 mg of Fe/g PVP, showing that ca. 77% of the initial Fe remained within the hydrogel. This result is expected since PVP is known to form stable complex with trivalent cations [26, 27]. Our procedure to reduce the Ferric ions by dialysis (see “Experimental section”) resulted in a nanogel containing only 16 µg of Fe/g PVP, as revealed by ICP-AES analysis.

Scanning electron micrographs of the collapsed PVP (freeze-dried) nanoparticles revealed spheres with mean diameter (D_m) of 27 nm, for the water swollen nanoparticles followed by freeze-drying (PVP-Fe^{3+}) D_m was 278 nm, and for nanogels submitted to dialysis and freeze-drying (PVP-iron free) D_m was 364 nm (Fig. 1). The calculated Q values are ~900 for PVP-Fe^{3+} nanogel and ~2,000 for PVP-iron-free nanogel. These Q values are 40 and 90 times larger than the value found for PVP macrogels

Table 1 Micellar diameters before and after crosslinking

Micelle core	Diameter (nm)
Water	11±2
PVP[a]	51±1
PVP[a]+$FeCl_2$[b]	78.2±0.5
PVP[a]+$FeCl_3$[b]	60±6
After crosslinking[c]	30.2±0.9

[a] 100 g×L^{-1}

[b] 7 mmol×L^{-1}

[c] By addition of 100 mmol×L^{-1} H_2O_2 in diethyl ether

Fig. 1 Scanning electron microscopy and diameter distribution of **a** collapsed PVP, **b** swollen and freeze-dried PVP-Fe^{3+}, and **c** submitted to dialysis and freeze-dried PVP-iron-free nanoparticles

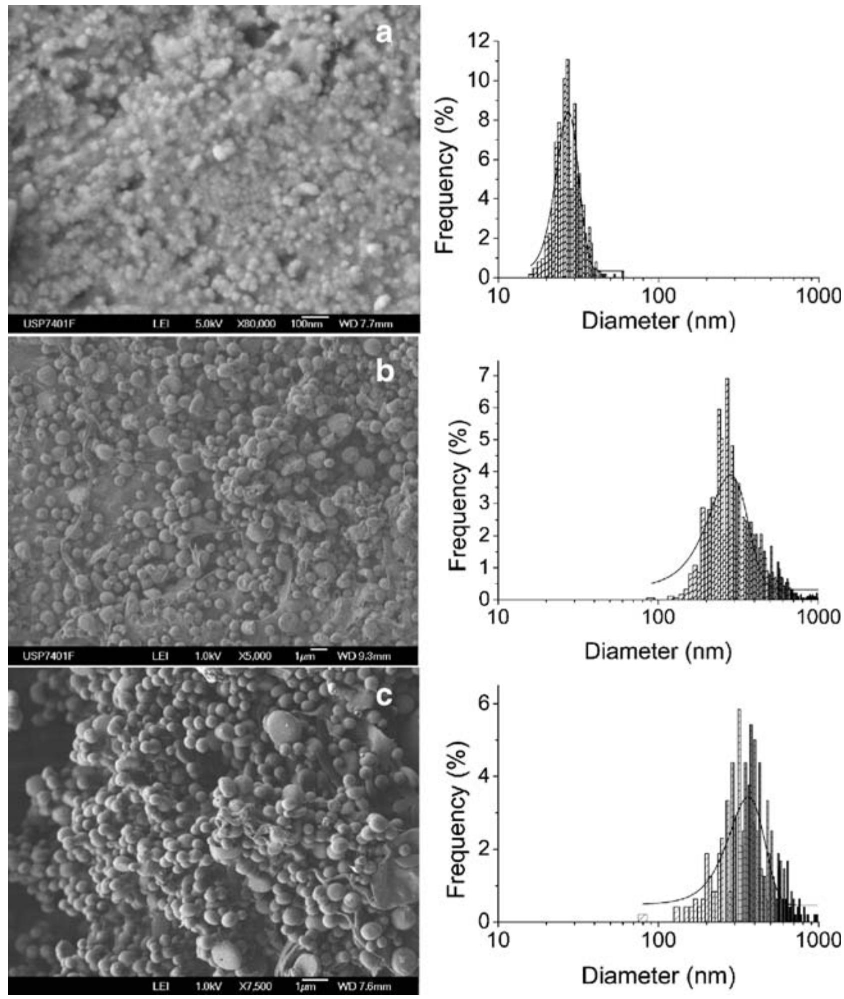

prepared by a similar method [17]. The nanometric size of the structure determines a swelling behavior similar to superabsorbent hydrogels.

Zeta Potential measurements evidenced marked changes in the surface charge of the nanogels when the Fe^{3+} ions are removed. The value of ζ for PVP-Fe^{3+} nanogels was +30 mV, while PVP-iron-free nanogels were uncharged at pH6.5 (Fig. 2).

Macrosized hydrogels with very low level of cross-linking are superabsorbents [20]. We have shown that the extent of crosslinking, ρ_x, can be correlated with anisotropy measurements of a fluorescent probe attached to the hydrogel network [28]. Static fluorescence polarization was measured in our preparations using probe amounts of a PVP copolymer containing anthracene residues, i.e., PVPVAn. The (low) anisotropy PVP–PVPVAn did not significantly change upon inclusion in reverse micelles (Table 2). The addition of ferrous and ferric ions in concentrations used in Fenton reaction (7 mmol$\times$L^{-1}), as expected in view of the known complexation reaction of PVP with metal cations [26], increased Γ up to twofold (Table 2). While addition of ferrous ions alone did not affect chemically the probe, further addition of H_2O_2 to attain Fenton conditions affects the anthracene moiety, with changes in excitation and emission characteristics of the probe (not shown). Changes in the probe did not affect the measurements of static anisotropy since the product presents is strong fluorescent. Using the same excitation–

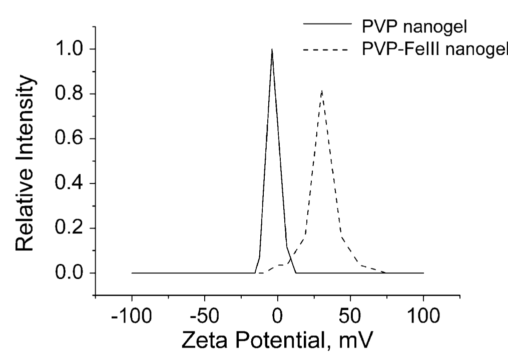

Fig. 2 Zeta Potential measurements for PVP-iron-free and PVP-Fe^{3+} nanogels in pH6.5

Table 2 Anisotropy (Γ) of PVP co-crosslinked with PVPVAn

Condition[a]	Γ
Solvent	0.041±0.007
CTAB	0.057±0.009
CTAB+$FeCl_2$	0.09±0.01
CTAB+$FeCl_3$[b]	0.11±0.02
After crosslinking	0.260±0.007

PVP/PVPVAn 1:1 (*w/w*); λ_{ex}=340 nm; λ_{em}=420 nm

[a] Otherwise stated, normal conditions used for nanogel preparation

[b] $[FeCl_3]$=7 mmol×L^{-1}

emission conditions, any changes in intensity are canceled (see Eq. 1). Fluorescence measurements were only taken after attaining constant fluorescence intensity after probe addition (ca. 30 min) to avoid equilibration artifacts. The total anisotropy after crosslinking doubled (Table 2) and was of the same order of magnitude of that measured for PVP macrogel [28]. As the Γ values of nano- and macrogels were similar and the PVP concentration were the same as that used previously (Fig. 2 of Ref. [28]), we conclude that both the macro- and nanogels have comparable degrees of crosslinking. Thus, the superabsorbing properties of these nanogels are unrelated to low levels of crosslinking.

The strong deswelling produced by increasing [NaCl] on the PVP-Fe^{3+} nanogel (Fig. 3) is typical of hydrogels prepared with polyelectrolytes [29–34]. The effect of increasing [NaCl] on the relative swelling of the PVP-Fe^{3+} nanogel was observed even at [NaCl]<1 M and reached a minimum Q/Q_0 (=0.1) above 1 M salt. The difference between the behavior of the PVP-Fe^{3+} and PVP-iron-free nanogels was striking, and even at 4.0 M salt, the value of Q/Q_0 for PVP-iron-free nanogel was only 0.5 (Fig. 3). The effect of pH on PVP-iron-free and PVP-Fe^{3+} nanogel swelling was also distinct and revealed a remarkable swelling ratio of more than 6,000 for PVP-iron-free nanogel

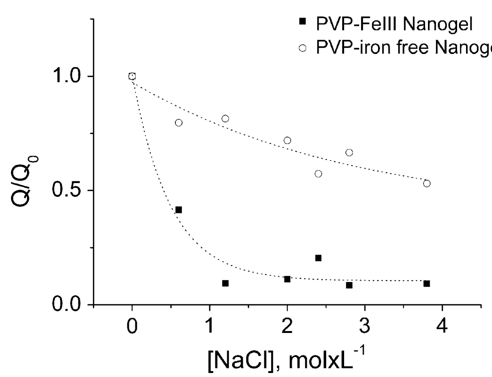

Fig. 3 Effect of salt concentration on nanogel relative swelling (Eq. 3)

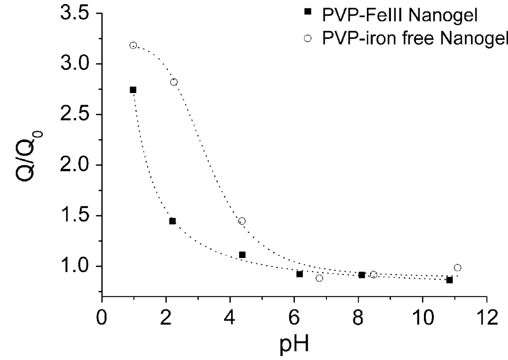

Fig. 4 Effect of pH on nanogels relative swelling (Eq. 3). The NaCl concentration (ionic strength) was fixed on 0.1 mol×L^{-1}, and the pH was controlled by HCl or NaOH addition

swollen in 1 M acid (Fig. 4). Swelling of PVP-Fe^{3+} nanogel approached that of PVP-iron-free nanogel below pH2, suggesting that H^+ could displace PVP-associated Fe^{3+}. Iron analysis of PVP-Fe^{3+} nanogel swollen at pH1.0 revealed that only 2% of the initial metal remained in the swollen nanogel (0.12 mg Fe/g PVP).

The deswelling of both PVP-iron-free and PVP-Fe^{3+} nanogels by salts follows the Hofmeister series, increasing with the capacity of anions to promote ordering in water structure (Fig. 5). Note that the deswelling effect is more pronounced with PVP-Fe^{3+}, a further indication of the polyelectrolyte nature of this nanogel. As a limit, both triflate and acetate salts coagulate PVP-Fe^{3+} nanogels (Fig. 5).

Discussion

Critical steps in the preparation of the PVP nanogels in reverse micelles are: (1) polymer inclusion, (2) the crosslinking reaction, (3) removal of the formatting system, and (4) removal of ferric ions. The choice of surfactant may influence all four steps. The Lewis base character of PVP makes the choice of cationic surfactants adequate to obtain higher stability of the micellar structure. A study of interaction of PVP with other micellar system (water/PVP/AOT/*n*-heptane [35]) shows that the polymer interacts directly with the ionic headgroup even when the surfactant is negatively charged. In our case, headgroup–PVP interactions can be assumed from the high solubility of the polymer in CTAB reverse micelles.

Although the addition of Fe^{2+} did not affect the solubility of PVP in the reverse micelles, a significant effect on the organization of the polymer inside the micelle was evident. The D_h of PVP-Fe^{2+} (or Fe^{3+})-containing reverse micelle prior to crosslinking were significantly larger than those with PVP (Table 1).

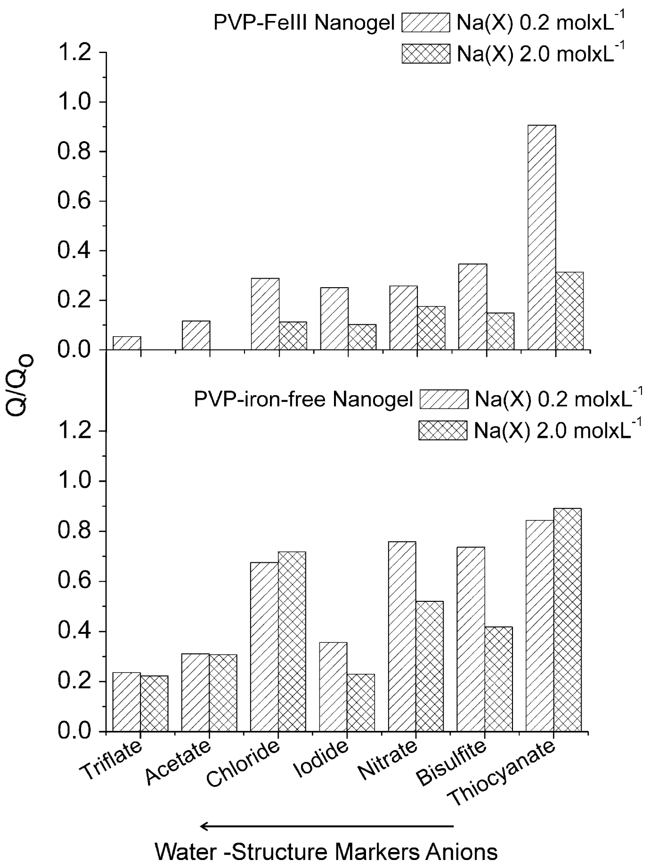

Fig. 5 Effect of different anions on the PVP nanogels diameter

Ferric ions complex with PVP with high affinity ($K = 6 \times 10^{11}$, [26]), imparting a polyelectrolyte character to the polymer. PVP has been proposed as a chelating agent in systems designed for removal and recovery of heavy metal ions [26]. To the best of our knowledge, the PVP-Fe^{2+} complex has not been described. However, most neutral carbonylic compounds complex Fe^{3+} with affinities that are larger than those with Fe^{2+}. Our results also indicate a strong binding of the ion to PVP. Charge–charge repulsion between ferrous or ferric ions bound to PVP may be responsible for D_h increase of the reverse micelle. Differences in binding constants to PVP may explain the differences in D_h's of the reverse micelles containing either Fe^{2+} or Fe^{3+}. Alternatively or synergistically, charge–charge repulsion between the cationic headgroups of the surfactant and the complexed Fe^{2+} ions may play an important role in determining D_h of micelles containing PVP-Fe^{2+} or PVP-Fe^{3+}.

Crosslinking was initiated with the addition of H_2O_2 dissolved in diethyl ether, leaving hydrogen peroxide to react with the ferrous ions in the water pool of the reverse micelles and initiate crosslinking. The mechanism of PVP radicalar crosslinking by Fenton reaction was proposed by Barros et al. [17]: The hydroxil radical generated by Fenton reaction abstracts hydrogen atoms from the PVP chain, generating macrorradicals, which can collapse, crosslinking the polymer. That article also describes the values of crosslinking density and mesh size for the macrogel, based on equilibrium swelling theory. Here, likewise, the nanogel stability against maximum swelling conditions demonstrates its covalent character.

Crosslinking was also attested by a reduction of D_h of PVP solution included in the micelle. DLS showed a decrease of 60% in its diameter, from 78 to 30 nm. This shrinking of the micelle cannot be accounted on the change of complexing cation since PVP-Fe^{3+}-containing reverse micelle is only 23% smaller than PVP-Fe^{2+}. Crosslinking of polymers in its dry state produces volume contraction due covalent coupling in adjacent chains [25, 36], and unpublished data from our laboratory show the same tendency with hydrated macrogels. Dry PVP films crosslinked with e-beam shrinks [36], and the swelling capacity depends upon crosslinking density. Here, the crosslinking promoted by Fenton reagent led to loss of structured, polymer-bound water, with consequent re-equilibration of PVP-micelle particle size. Differences in water properties in the aqueous pool of reverse micelles are widely documented [37, 38].

The Q of purified PVP-Fe^{3+} nanogels (>900) was significantly higher than that of the PVP macrogel [28]. The Q value for PVP macrogels produced by the same process is 23, comparable to other macrogels [28, 39]. The Q value of 900 obtained here is in the high range of swelling ratios described for other nanogels [40, 41].

Iron-free PVP nanogels were strikingly different in swelling behavior. In distilled water, the value of Q for PVP nanogels, estimated by scanning electron microscopy, was above 2,000. Crosslinked hydrophilic polymers are considered superabsorbent (or SAPs) when Q values lie from 10 to 1,000 [40]. Superabsorbent behavior is observed in core-shell nanogels [5]. The maximum Q with PNIPAAm/poly(2-vynilpyridine) is 1,300. Pluronic/heparin nanocapsules [40] present a thermally controlled Q of 1,000, and Q values of 1,500 and 2,000 are characteristic of modified-carrageenan and anionic acrylamide-based hydrogels [42, 43]. The high value of Q of PVP is not attributable to low crosslinking as we showed by measuring anisotropy-related properties (see "Results").

The balance between elastic forces of the polymer network and osmotic pressure due the presence of free counter ions of the polymer-bound Fe^{3+} should determine the swelling characteristics of the nanogel. The increase in the ionic strength led to shrinking of the nanogel by reducing osmotic pressure (Fig. 3) [44]. PVP-iron-free nanogel shrinking by NaCl is small compared to PVP-Fe^{3+} nanogel and must have a different origin. Here, the structure of the swollen gel relies exclusively on the water organization around the polymer, more specifically around the pyrrolidone moieties. The salt effect on Q/Q_0 of PVP-iron-free nanogels is smaller, implying a different mechanism. Salt-induced shrinking of polymeric hydrogels is well characterized and charged, and neutral hydrogels exhibit different swelling behaviors. Anionic acrylamide-based hydrogels shrink with NaCl as do PNIPAAm/poly(2-vinylpyridine) core-shell nanogels [5, 42]. The effect of salt is higher in the charged form of poly(HEMA-*co*-AA) hydrogel [44]. Similarly, Q of acrylamide-based polyampholyte hydrogel becomes more sensitive to ionic strength as the charge of the polymer increases [45]. The behavior of Q of hydrogels with ionic strength is attributed to the binding of water molecules to ions associated with polymer segments, changing the hydrophobic interactions and shrinking the nanogel, i.e., an effect of competition by solvation water molecules between polymer and ion.

Salt addition to swollen PVP macrogel produces shrinking that depends on the nature of the anions/cations. A model based on hydration of pyrrolidone carbonyl rather than that of hydrophobic regions of the polymer explains this ion-specific Q behavior [46]. This model considers two different types of hydrogen bonding with water molecules via electron-pair acceptance (EPA) or donation (EPD) abilities, which can be modified by the added cation or anion. Hydration destabilization leads to deswelling (salting-out) and is promoted by decrease of EPA or increase of EPD ability of water. In this series of studied anions, Cl^- is of moderate intensity, corroborating the NaCl effect upon the PVP-iron-free nanogel here observed.

The ion-specificity effect (lyotropic series) on swelling behavior of neutral hydrogels has been observed with other hydrogels. The sol–gel thermal phase transition of hydroxypropylmethylcellulose is influenced by anions that affect water structure [47]. The shrinking of poly(ethylene oxide) hydrogels is less prominent with Cl^-, Br^-, and I^- and very strong with SO_4^{2-} [48]. Poly(vinyl alcohol) hydrogels have the same behavior [49], shrinking in anions that strongly

Scheme 2 **a** PVP-Fe^{3+} nanogels scheme of Fe^{3+} complex crosslinking. **b** PVP-iron-free scheme of protonation of polymeric chains

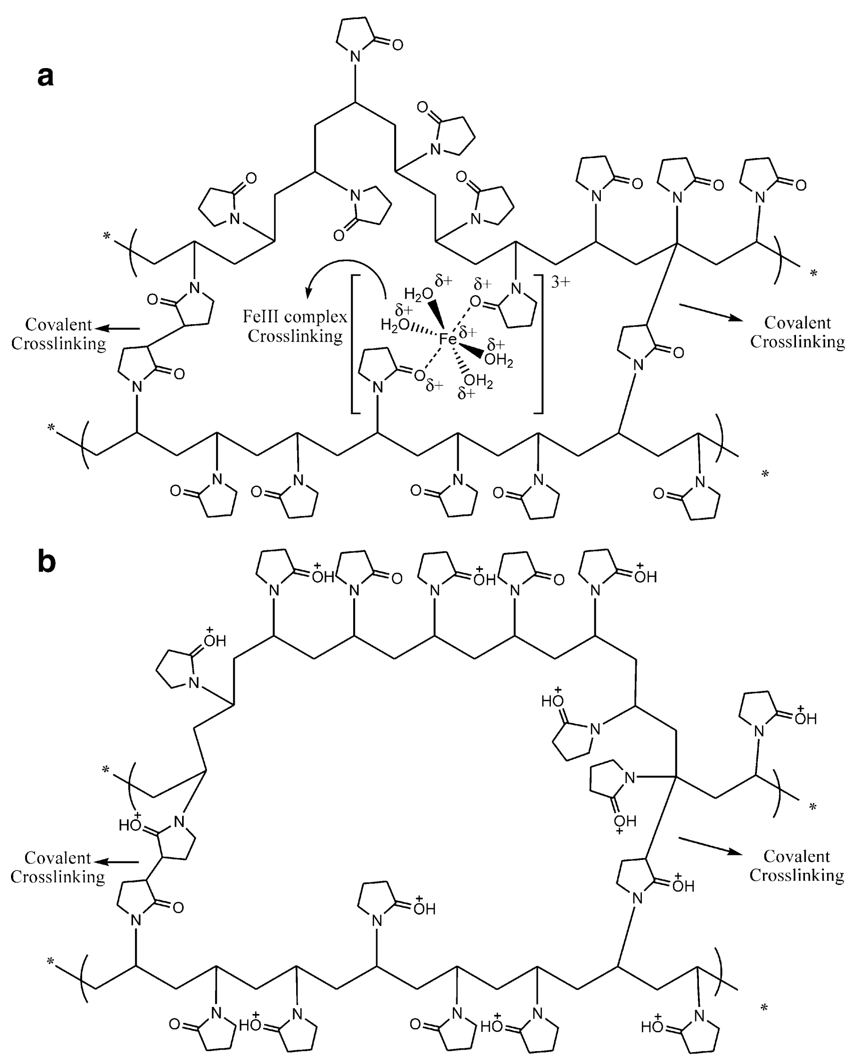

interact with water. Hydrogel systems composed by polyelectrolytes have also been studied. Poly(acrylic acid) hydrogel contract with the addition of strongly hydrated ion [50]. Hydroxypropylmethyl cellulose phthalate shrinks with salt ($Br^{-}>SCN^{-}>Cl^{-}>F^{-}$), and the effect is more prominent with strongly hydrated anions [51]. An inverse relationship between swelling and water binding ability of a cation is found with modified carrageenan, where the ability of complexation of the large cations with carrageenan, increasing the crosslinking degree, appears to be the cause of the specificity [43]. This effect is inverse for hydrolyzed carrageenan, which contains carboxylate moieties that can interact strongly with small cations [43]. Salt-induced shrinking of poly(styrene sulfonic acid) hydrogel follows the lyotropic series of anions [52].

The magnitude of the anion effects on Q/Q_0 of PVP nanogels (Fig. 4) partly coincides with the series described studying anion effects on macrogel swelling, only the SCN^{-}/I^{-} relative positions differ [46]. The ion specificity here observed follows typical Hofmeister orders, i.e., $SCN^{-} < HSO_3^{-} < NO_3^{-} < I^{-} < Cl^{-} < AcO^{-} < TfO^{-}$. Large anions, such as the water-structure breaking SCN^{-}, make hydrophobic hydration more favorable. With PVP-Fe^{3+} nanogels, all anions induce deswelling, including large anions like SCN^{-}, HSO_3^{-}, and NO_3^{-}. At the limit, PVP-Fe^{3+} collapses at high TfO^{-} concentration and coagulation can be observed (not shown). Salt specificity effects on deswelling of PVP-Fe^{3+} cannot be correlated with anion binding to PVP-bound Fe^{3+} since the effects are clear even for anions that knowingly complex very weakly with this ion. In particular triflate, the anion with the highest deswelling effect does not form complexes with Fe^{3+} [53]. In the case of PVP-Fe^{3+} nanogels, specific salt effects can be best accommodated by the interaction between anion and water [42]. Hydration of PVP-Fe^{3+} nanogels requires more water to maintain solvated Fe^{3+}.

Hydrogels and nanogels swelling can be influenced by the pH of the media [5, 50]. Groups that can ionize or protone such as poly(acrylic acid) [50] or PNIPAAm/poly(2-vinylpyridine) [5], respectively, account for swelling pH dependence. In the case of PVP nanogels, the amide groups can be protoned. Protoned positively charged chains will repel each other, explaining the increase in swelling ratio for the nanogels. The maximum swelling ratio depends on the maximum stretching of the polymeric chains, which may be, in the case of produced PVP nanogels, near Q=6,000 (Scheme 2b). It is attractive to propose that charge–charge repulsion in Fe^{3+}-containing PVP nanogels is compensated by intramolecular reticulation due to Fe complexation with the numerous N and C═O present on the polymer chain (Scheme 2a). As H^{+} displaces the bound Fe^{3+}, the dominant effect is charge–charge repulsion and the swelling increases accordingly.

Conclusion

Nanogel particles were obtained by crosslinking of PVP included in reversed micelles using Fenton reaction. Because of the preparation procedure, the detergent-free nanoparticles contain bound Fe^{3+} (PVP-Fe^{3+}), and the particles exhibit typical polyelectrolyte-like behavior. Dry PVP-Fe^{3+} nanoparticles (diameter=27 nm) swell in water (278 nm) and exhibit a swelling ratio (Q) of ca. 900. Fe^{3+} ion removal by acidification and dialysis yields essentially PVP-iron-free nanoparticles showing Q values of 2,000, a property characteristic of superabsorbent hydrogels. Cross-linking densities of the PVP-Fe^{3+} nanoparticles, assessed by anisotropy measurements, are of the same order as those obtained for PVP macrogels. The swelling of the PVP-iron-free nanogels varied with salt concentration, following the lyotropic series of anions. At pHs lower than 1.5 these nanogels exhibit an extremely high Q value of 6,000.

Acknowledgment We thank the Brazilian Agencies Fundação de Amparo à Pesquisa do Estado de São Paulo (FAPESP) and Conselho Nacional de Desenvolvimento Científico e Tecnológico (CNPq) for the financial support.

References

1. Rosiak JM, Yoshii F (1999) Nucl Instrum Methods Phys Res, Sect B 151:56–64
2. Panyam J, Labhasetwar V (2003) Adv Drug Delivery Rev 55:329–347
3. Otsuka H, Nagasaki Y, Kataoka K (2003) Adv Drug Delivery Rev 55:403–419
4. Daoud-Mahammed S, Couvreur P, Gref R (2007) Int J Pharm 332:185–191
5. Kuckling D, Vo CD, Wohlrab SE (2002) Langmuir 18:4263–4269
6. Vo CD, Kuckling D, Adler H-JP, Schonhoff M (2002) Colloid Polym Sci 280:400–409
7. Gaur U, Sahoo SK, De TK, Ghosh PC, Maitra A, Ghosh PK (2000) Int J Pharm 202:1–10
8. McAllister K, Sazani P, Adam M, Cho MJ, Rubinstein M, Samulski RJ, Desimone JM (2002) JACS 124:15198–15207
9. Brannon-Peppas L (1997) Med Plast Biomater 4:34–44
10. Vinogradov SV, Bronich TK, Kabanov AV (2002) Adv Drug Delivery Rev 54:135–147
11. Bharali DJ, Sahoo SK, Mozumdar S, Maitra AJ (2003) Colloid Interface Sci 258:415–423
12. Aliyar HA, Hamilton PD, Remsen EE, Ravi NJ (2005) Bioact and Compat Polym 20:169–181
13. Sahiner N, Godbey WT, Mcpherson GL, John VT (2006) Colloid Polym Sci 284:1121–1129
14. Ulanski P, Janik I, Rosiak JM (1998) Radiat Phys Chem 52:289–294
15. Rosiak JM, Janik I, Kadlubowski S, Kosicki M, Kujawa P, Stasica P, Ulanski P (2003) Nucl Instrum Methods Phys Res Sect B 208:356–360
16. Neyens E, Baeyens J (2003) J Hazard Mater B 98:33–50
17. Barros JAG, Fechine GJM, Alcantara MR, Catalani LH (2006) Polymer 47:8414–8419

18. Leger C, Nguyen QT, Neel J, Streicher C (1995) Macromolecules 28:143–151
19. Valeur B (2002) Molecular Fluorescence: Principles And Application, 2nd ed . Wiley, NY, USA
20. Peppas NA, Barr-Howell BD (1986) Characterization of the cross-linked structure of hydrogels. In: Peppas NA (ed) Hydrogels in medicine and pharmacy. Volume I: fundamentals. CRC, Boca Raton, pp 27–56
21. Miyazaki T, Yoshioka S, Aso Y (2006) Chem Pharm Bull 54:1207–1210
22. Bellows RJ, King CJ (1972) Cryobiology 9:559–561
23. Hiemens PO (1986) Principles of colloids and surface chemistry, 2nd edn. Marcel Dekker, New York, p 815
24. Liu M, Yan X, Liu H, Yu W (2000) React Funct Polym 44:55–64
25. Jeong U, Ryu DY, Kim JK, Kim DH, Russell TP, Hawker CJ (2003) Adv Mater 15:1247–1250
26. Çaykara T, Inam R, Öeztüerk Z, Güeven O (2004) Colloid Polym Sci 282:1282–1285
27. Biedermann HG, Graf WZ (1975) Naturforsch, B: Anorganische Chemie, Organische Chemie 30:226–228
28. Fechine GJM, Barros JAG, Alcantara MR, Catalani LH (2006) Polymer 47:2629–2633
29. Zhao Y, Chen W, Yang Y, Yang X, Xu H (2007) Colloid Polym Sci 285:1395–1400
30. Feng X, Pelton R (2007) Macromolecules 40:1624–1630
31. Xu S, Cao L, Wu R, Wang J (2006) J Appl Polym Sci 101:1995–1999
32. Chiu H-C, Lin Y-F, Hung S-H (2002) Macromolecules 35:5235–5242
33. Jeon CH, Makhaeva EE, Khokhlov AR (1998) Macromol Chem Phys 199:2665–2670
34. English AE, Tanaka T, Edelman ER (1996) J Chem Phys 105:10606–10613
35. Luan Y, Xu G, Dai G, Sun Z, Liang H (2003) Colloid Polym Sci 282:110–118
36. Burkert S, Schmidt T, Gohs U, Moench I, Arndt K-F (2007) J Appl Polym Sci 106:534–539
37. Politi MJ, Chaimovich H (1986) J Phys Chem 90:282–287
38. Khougaz K, Gao Z, Eisenberg A (1997) Langmuir 13:623–631
39. Yu Y-Q, Xu Y, Ning H, Zhang S-S (2008) Colloid Polym Sci 286:1165–1171
40. Choi SH, Lee J-H, Choi S-M, Park TG (2006) Langmuir 22:1758–1762
41. Akiyama Y, Fujiwara T, Takeda S-I, Izumi Y, Nishijima S (2007) Colloid Polym Sci 285:801–807
42. Okay O, Sariisik SB, Zor SD (1998) J Appl Polym Sci 70:567–575
43. Hosseinzadeh H, Pourjavavdi A, Zohuriaan-Mehr MJ (2004) J Biomater Sci, Polym Ed 15:1499–1511
44. Khare AR, Peppas NA (1995) Biomaterials 16:559–567
45. Baker JP, Stephens DR, Blanch HW, Prausnitz JM (1992) Macromolecules 25:1955–1958
46. Takano M, Ogata K, Kawauchi S, Satoh M, Komiyama J (1998) Polymer Gels and Networks 6:217–232
47. Liu SQ, Joshi SC, Lam YC (2008) J Appl Polym Sci 109:363–372
48. Masuda Y, Nakanishi T (2002) Colloid Polym Sci 280:547–553
49. Masuda Y, Okazaki Y, Nakanishi T (2002) Colloid Polym Sci 280:873–875
50. Muta H, Kawauchi S, Satoh M (2003) Colloid Polym Sci 282:149–155
51. Xu L, Yue Z, Wang M, Zhai M, Yoshii F, Seko N, Peng J, Wei G, Li J (2007) Nucl Instrum Methods Phys Res, Sect B 265:394–398
52. Xu L, Li X, Zhai M, Huang L, Peng J, Li J, Wei G (2007) J Phys Chem B 111:3391–3391
53. Liu W, Etschmann B, Brugger J, Spiccia L, Foran G, McInnes B (2006) Chem Geol 231:326–349